# IFU in the era of TMT : Kinematics of distant star-forming galaxies


Marie Lemoine-Busserolle (Gemini Observatory)

Co. : F. Lamareille (LA2T, France), A. Bunker (University of Oxford, UK), M. Kissler-Patig (Gemini Observatory) &S.F. Sanchez (CSIC-MPI, Spain)


## AIM

*Optical/near-IR integral field (or 3D) spectroscopy is now a well developed field, with integral field units (IFUs) being operated on a large number of ground- and space-based telescopes. With IFUs being planned for next-generation ELTs (GMT, TMT, E-ELT), we are now in the era of IFUs. The time is therefore ripe to review the current science focusing on spatially resolving galaxies being done with integral field spectrographs, in particular the study of the mass-assembly histories of galaxies which have been recently the focus of many studies at redshift 1 to 3. Indeed the kinematics of distant galaxies, from z = 1 to z > 2, play a key role in our understanding of galaxy evolution from early times to the present. Internal kinematics tell us directly about the dynamical state of galaxies, reveal the potential well depths of individual galaxy–dark-matter halo systems, probe the intrinsic, or local, velocity dispersion of a galaxy, which allows one to quantify the degree of non-circular motions such as pressure support, and can be measured for a large sample of galaxies over a significant range in redshift. Here I show the state-of-the-art IFU studies of distant star-forming galaxies which reveal a kinematic mixture of objects displaying ordered rotational motions, and also fairly large velocity dispersions. I also present results obtained from Integral Field NIR Spectroscopy with SINFONI/VLT of a sample of 13 high-z (1 < z < 4) star-forming galaxies (4<230 M⊙/yr) selected from the VIMOS/VLT Deep Survey (VVDS). And briefly present also an interesting result obtained for a comparable star-forming "chain" galaxy (A370-A5, z=1.341) discovered as an arc behind the lens cluster Abell 370 (z=0.374). Finally I presented a new instrument, SAMI for the ATT which, makes use of astrophotonic technology in the form of hexabundles (multi-core fibre bundles) to enable simultaneous IFU observations of 13 objects over a 1-degree diameter accessible field.*

### Galaxy Kinematics at High Redshift - How?

*At z < 1.5 : velocity fields obtained with optical spectrographs, [OII]3727 emission line is still visible. At higher redshifts (1.5 < z < 3.5), NIR observations are mandatory: [OII] in J, Hβ & [OIII] in H band, Hα in K band.*

*Long-slits have strong limitations and integral-field spectrographs (IFU) are better to derive accurate velocity fields.*

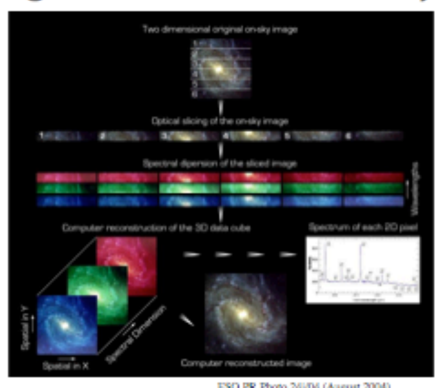

## STATE-OF-THE-ART OF KINEMATICS STUDIES FROM IFU data

**Compilation of most kinematic measurements of galaxies over 0.1<z<4**

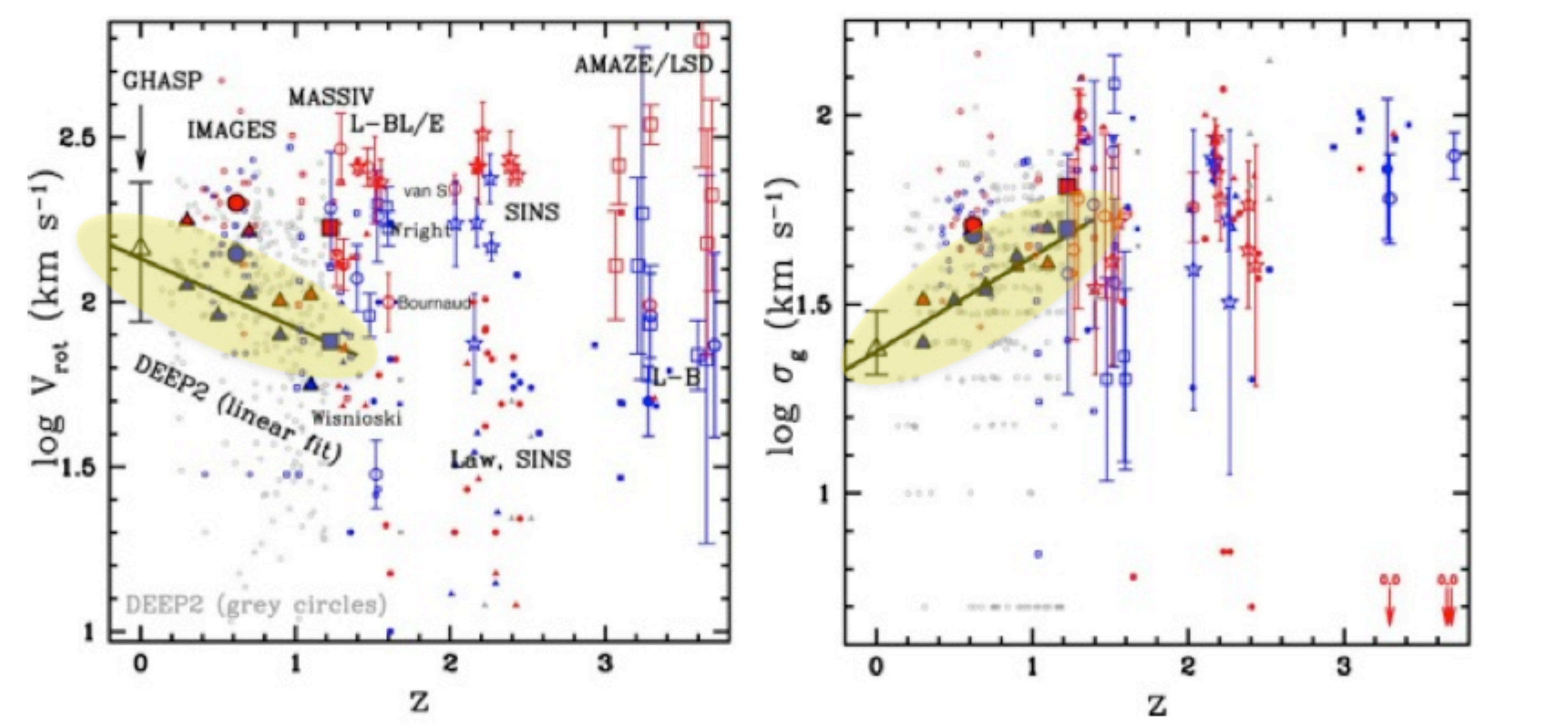


Log $M_*$ (Msun) > 10.3 Large open symbols = disk model fit

Log $M_*$ (Msun) < 10.3 Small filled symbols = delta V used

Large filled symbols = medians in z

***No trends with redshift beyond z~1.5 !*** **Kassin et al. (2012b)**

## SOME RESULTS USING SINFONI-VLT

### sample @ 1 < z < 1.6

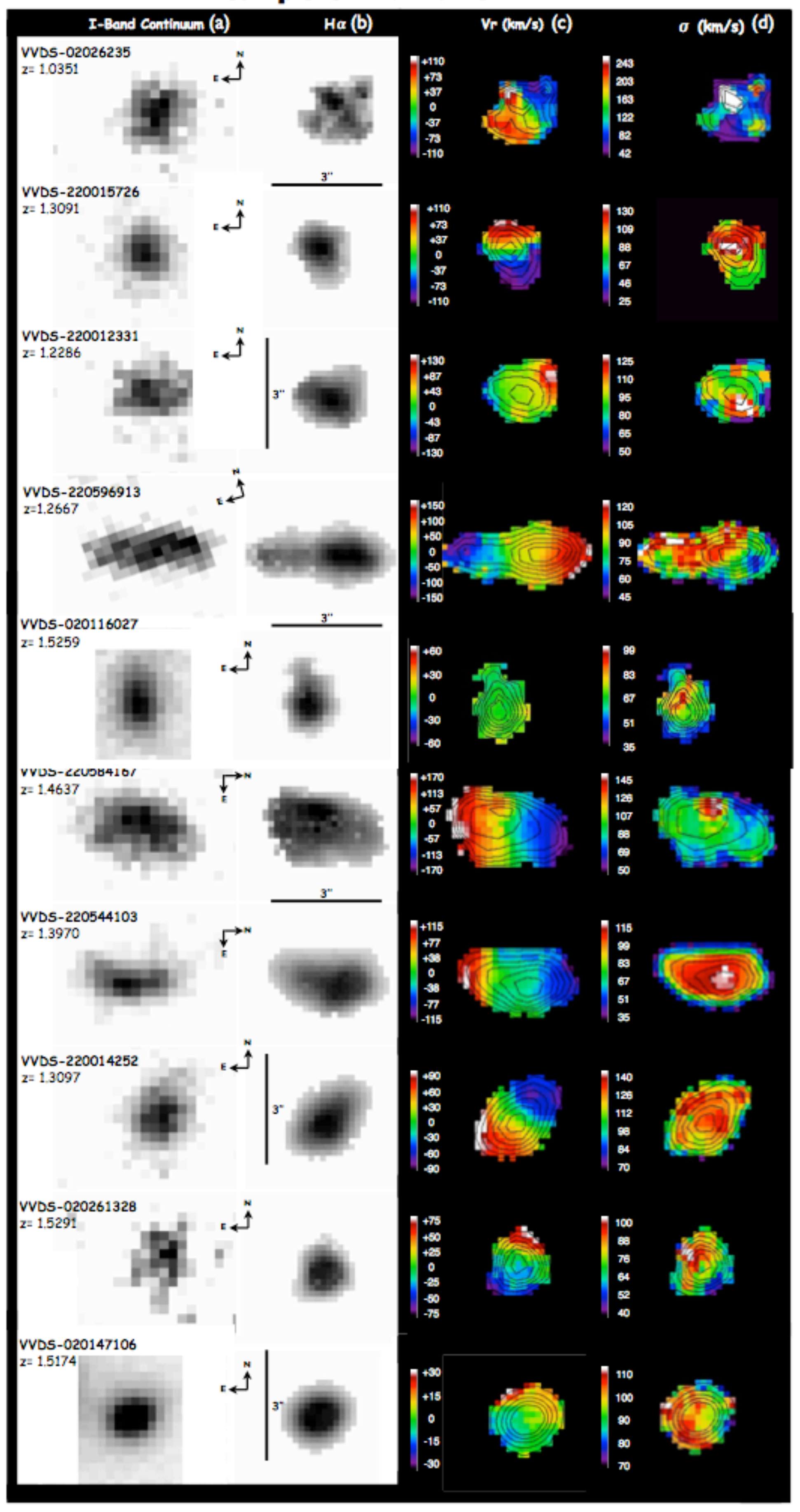

*From left to right: (a) I-band CFHT image; (b) Hα flux map; (c) Hα velocity field and (d) Hα velocity dispersion map obtained from Gaussian fits to the data cubes after smoothing spatially with a 2D Gaussian of FWHM = 3 pixels. The I-band image and Hα maps are color coded with a linear scaling such that the values increase from light to dark. These data have been acquired with the 125 × 250 mas sampling configuration of SINFONI/VLT, in seeing-limited mode. An angular size of 1 arcsec corresponds to ~8 kpc at the redshifts of most of the objects.*

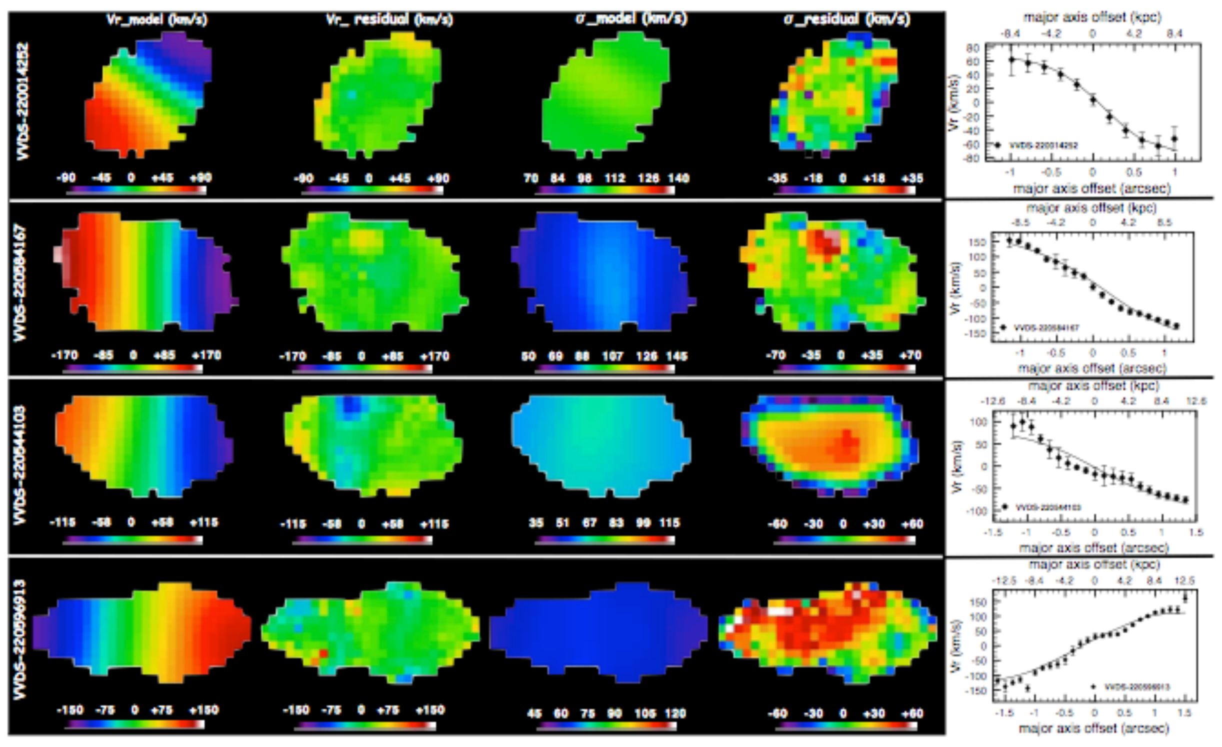

*Kinematic best-fitting models of galaxies of our sample (left-hand panel) for both the velocity and the dispersion, after adding the effect of the beam smearing. The difference for both the velocity and the dispersion between the observed map and the best-fitting model map is also shown and may display non-negligible random motions in the gas. A 1D rotation curve extracted using an 'idealized' slit from the observed Hα velocity map, overlaid with the best-fitting model, is shown in the right-hand panel.*

| Galaxy | $M_\star$ (1) | $z_{H\alpha}$ | SFR $^0_{UV}$ (3) | SFR $_{SED}$ (4) | $E(B-V)_{SED}$ (5) | Age (6) | SFR $_{corr}$ (5) | $M_{gas}$ (7) | $\mu$ (8) | $V_{rot}/\sigma_0$ | $M_{vir}$ (1) | $M_{dyn}$ (1) | $\frac{r_c}{r_{gas}}$ | $Q$ (2) | Dyn. class (3) |
|---|---|---|---|---|---|---|---|---|---|---|---|---|---|---|---|
| VVDS-1235 | 6 ± 2 | 1.0352 | 1.8 ± 0.2 | 11 ± 5 | 0.28 ± 0.12 | 0.68 ± 0.3 | 8.8 ± 1 | 8.4 ± 0.7 | 0.58 ± 0.08 | – | 4 ± 2 | – | – | – | Merger |
| VVDS-2331 | 11 ± 3 | 1.2286 | 3 ± 0.1 | 27 ± 14 | 0.32 ± 0.11 | 0.54 ± 0.3 | 42 ± 8 | 31 ± 4 | 0.74 ± 0.06 | 5.1 ± 2.9 | 6.4 ± 2.9 | 0.4 ± 0.7 | 0.52 ± 0.87 | 3.3 ± 0.9 | RD |
| VVDS-6913 | 43 ± 16 | 1.2660 | 7.1 ± 0.4 | 49 ± 22 | 0.28 ± 0.10 | 0.96 ± 0.5 | 17 ± 2 | 22 ± 2 | 0.34 ± 0.09 | 3.2 ± 0.8 | 20 ± 6.5 | 5 ± 3 | 0.53 ± 0.15 | 2.4 ± 0.6 | DD |
| VVDS-5726 | 50 ± 17 | 1.2927 | 2.4 ± 0.4 | 42 ± 28 | 0.37 ± 0.13 | 1.26 ± 0.7 | 23 ± 2 | 19 ± 1 | 0.28 ± 0.07 | 4.9 ± 0.5 | 8.7 ± 0.3 | 3 ± 4 | 0.22 ± 0.3 | 3.3 ± 0.5 | RD |
| VVDS-4252 | 21 ± 7 | 1.3099 | 9.4 ± 0.2 | 73 ± 26 | 0.28 ± 0.08 | 0.40 ± 0.2 | 280 ± 83 | 143 ± 30 | 0.87 ± 0.04 | 1.3 ± 0.1 | 14 ± 8.7 | 2 ± 1 | 0.42 ± 0.19 | 0.4 ± 0.7 | DD |
| VVDS-4103 | 16 ± 4 | 1.3966 | 7.7 ± 0.4 | 91 ± 49 | 0.28 ± 0.03 | 1.75 ± 1.6 | 412 ± 108 | 208 ± 39 | 0.93 ± 0.02 | 2.0 ± 0.7 | 12 ± 13 | 3 ± 2 | 0.63 ± 0.23 | 0.3 ± 0.8 | DD |
| VVDS-4167 | 25 ± 8 | 1.4656 | 10.6 ± 0.4 | 129 ± 46 | 0.29 ± 0.07 | 0.29 ± 0.1 | 28 ± 1 | 34.1 ± 0.8 | 0.58 ± 0.08 | 4.8 ± 0.8 | 26 ± 2.2 | 17 ± 5 | 0.65 ± 0.13 | 7.5 ± 0.5 | RD |
| VVDS-7106 | 8 ± 2 | 1.5194 | 10.6 ± 0.1 | 44 ± 11 | 0.16 ± 0.04 | 0.27 ± 0.1 | 16 ± 2 | 16 ± 1 | 0.67 ± 0.06 | 1.3 ± 0.4 | [illegible]1 ± 0.7 | [illegible] ± 3 | 1.22 ± 0.58 | [illegible].4 ± 1.0 | DD |
| VVDS-6027 | 11 ± 4 | 1.5301 | 4.1 ± 0.2 | [illegible] ± 12 | 0.24 ± 0.08 | 0.46 ± 0.3 | 3.9 ± 0.4 | 5.5 ± 0.4 | 0.33 ± 0.08 | – | [illegible]1 ± 0.5 | – | – | – | I.I. |
| VVDS-1328 | 11 ± 6 | 1.5289 | 3.5 ± 0.2 | 14 ± 6 | 0.19 ± 0.11 | 0.88 ± 0.6 | 3.9 ± 0.5 | 5.7 ± 0.5 | 0.34 ± 0.12 | 5.1 ± 0.7 | 3.4 ± 1.0 | 0.4 ± 3 | 0.07 ± 0.56 | 5.7 ± 0.7 | RD |

(1) (2) (3) (4) (5) (6) (7) (8) (9) (10) (11) (12)

*The columns are : (1) stellar mass (10^9 M⊙); (2) raw SFR from UV luminosity (M⊙ yr−1); (3) deredenned SFR from the SED; (4) reddening suffered by the stars; (6) age of the oldest stellar populations (Gyr); (6) dereddened SFR; (7) gas mass (10^9 M⊙); (8) gas mass fraction; (9) viral mass and (10) dynamical mass (10^9 M⊙); (11) the Toomre parameter (Toomre 1964); (12) dynamical class.*

### sample @ z ~ 3.5

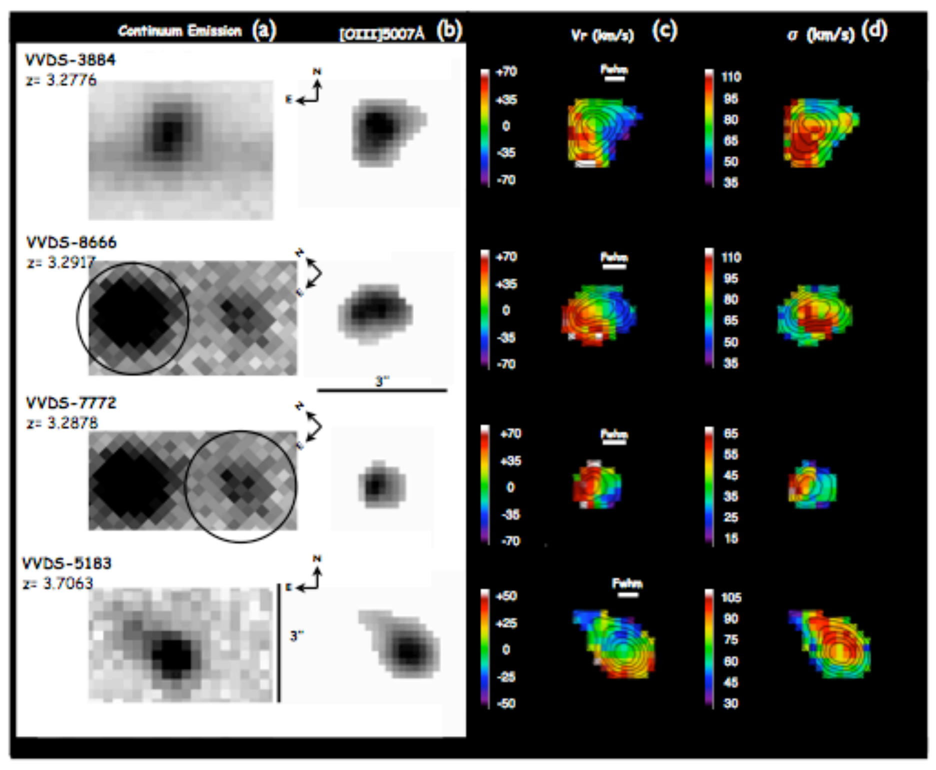

*From left to right: (a) CFHTLS image (r-band for VVDS-3884, VVDS-8666 and VVDS-7772; i-band for VVDS-5183), (b) [O III] λ5007 flux map, (c) [O III] λ5007 velocity field and (d) [O III] λ5007 velocity dispersion map obtained from Gaussian fits to the SINFONI data cubes after smoothing spatially with a 2D Gaussian of FWHM = 3 pixels.*

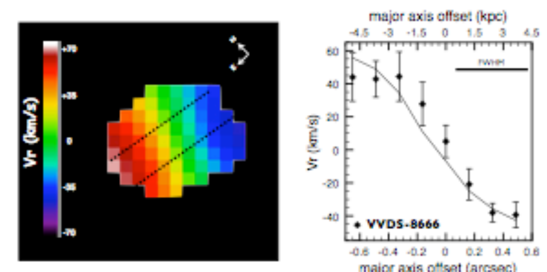

*2D disc model after convolution with a 0.58 arcsec PSF for VVDS-8666 (left-hand panel). 1D rotation curve (right-hand panel; full diamond), overlaid with the best-fitting model (solid line).*

| Galaxy | $SFR^0_{neb}$ (8) | $E(B-V)_{gas}$ (9) | $SFR_{neb}$ (10) |
|---|---|---|---|
| VVDS-3884 | 125 ± 4 | 0 | 125 |
| VVDS-8666 | 97 ± 19 | 0.35 | 427 |
| VVDS-7772 | <5.1 (2σ) | 0 | <5.1 |
| VVDS-5183 | 231 ± 57 | 0.40 | 1257 |

*(8) raw SFR from the nebular emission luminosity (M⊙ yr−1); (9) reddening suffered by the gas; (10) dereddened SFR.*

### All galaxies @ 1 < z < 3.5

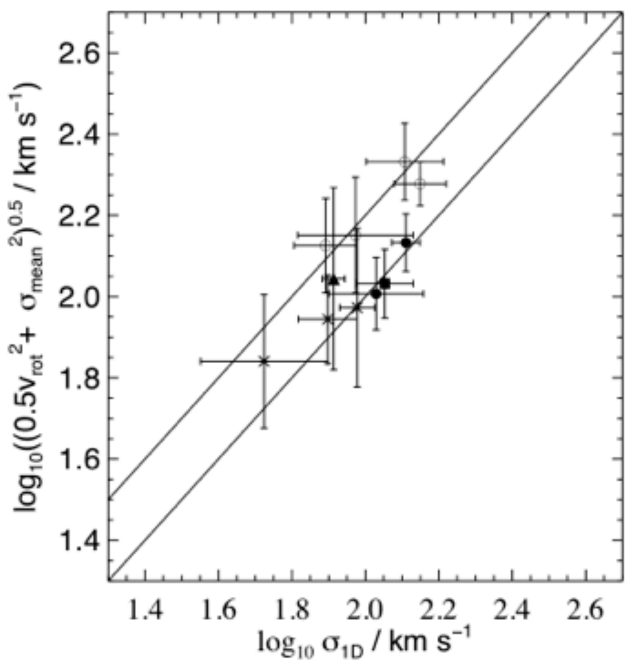


*Combined velocity (S0.5) versus integrated line-width velocity dispersion. The symbols are open circle – RD rotating discs, and filled symbols – DD rotating discs with in particular filled triangle (VVDS-7106) and filled squares (VVDS-6913); asterisk – z ~ 3 galaxies. This plot which give an idea of the evolution of the dynamical mass which takes also into account the contribution from the random motions in the gas shows an increase of the dynamical mass for z ~ 3–4 to 1.3–1.5 for the DD discs.*

## The Sydney-AAO Multi-object Integral field spectrograph

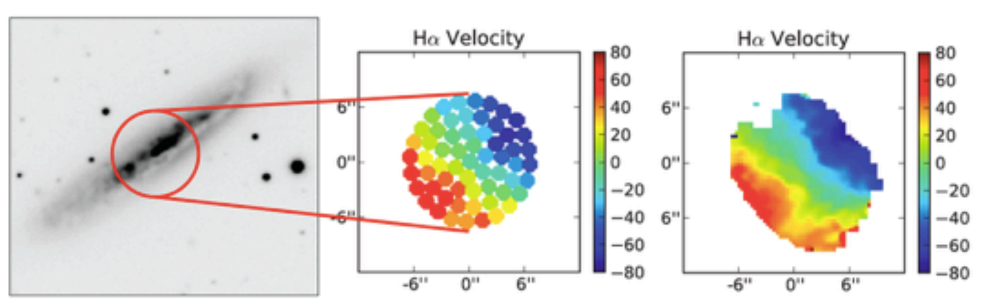


**SAMI is the Sydney Australian Astronomical Observatory Multi-object Integral Field Spectrograph, a brand new instrument on the 4-meter Anglo-Australian Telescope at Siding Spring Observatory.**

*Integral field spectroscopy has almost exclusively been limited to single-object instruments, meaning that it is time-consuming to build large samples. the first fully operational demonstrator instrument to use hexabundles. Hexabundles (Bland-Hawthorn et al. 2011; Bryant et al. 2011) are optical fibre bundles where the cladding has been stripped from each fibre to a minimum over a short length (~30 mm) and the fibres then gently fused together at the input end to provide an IFU (~1 mm aperture) with high filling factor. These can then be used in conventional multi-fibre spectrographs. SAMI has 13 IFUs that can be positioned anywhere over a 1-degree diameter FoV.*

sami galaxy survey

*The SAMI Galaxy Survey began in March 2013, with the intention of creating a large survey of 3000 galaxies across a large range of environment. The key science goals of the SAMI Survey are to answer the following questions:*

- *what is the physical role of environment in galaxy evolution?*
- *What is the relationship between stellar mass growth and angular momentum development in galaxies?*
- *How does gas get into and out of galaxies, and how does this drive star formation?*


- Lemoine-Busserolle et al. 2010, MNRAS 401, 1657

-Lemoine-Busserolle & Lamareille 2010, MNRAS 402, 2291


GEMINI OBSERVATORY

## MAGNIFICATION FROM LENS CLUSTER HELP !

**2D kinematics of lensed arc A5 (z=1.341) in the core of A370.**

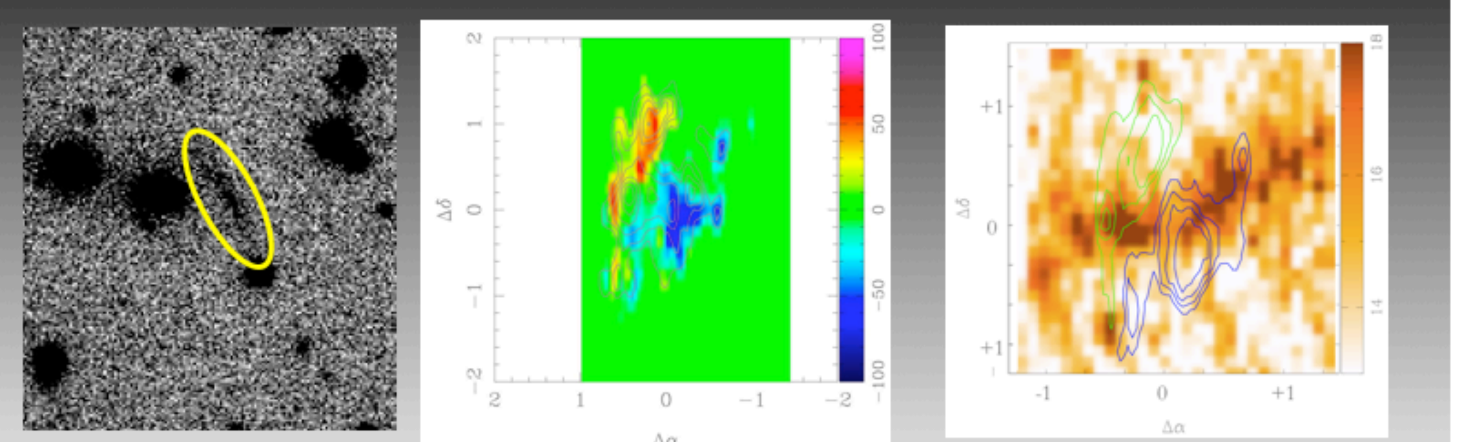

*Center: Hα velocity map in km/s obtained by fitting the emission line of each spectrum to a single gaussian function with the Hα intensity overlaid as contours. The lensing distortion has been removed. Images are oriented North-East, with the scale is acsecs. Contours show the Hα flux intensity. Right: Grayscale of the F336W-band image corresponding to the rest-frame UV emission (λ = 1435 Å) obtained using WFPC 2 on HST with the Hα velocity map overlaid as contours. The approaching velocities are in blue and the receding ones in green. Kinematics are consistent with a bipolar outflow with a range of velocities of v~100 km/s (work in progress).*

## WHAT TO REMEMBER ?

*NIR-IFU provides spatially resolved galaxy dynamics using bright rest-frame optical emission lines, allowing statistical studies of dynamical masses, SFRs, Tully-Fisher relations and metallicities. Using this data, we can set constrains on the formation and evolution of star-forming galaxies, during an epoch of when we expect strong evolution in their masses and mass-to-light ratios. Up to now studies of galaxy kinematics at z > 1.5 show few clear trends with redshift, likely due to sample selection since only the most highly star-forming systems at these redshifts can currently be studied, but also due to instrumental artifacts and observational conditions. However, it is clear that high-z galaxies have a significant amount of disordered motions, whether or not they show evidence of rotation. In addition, the study of lensed galaxies allows to probe a low mass regime of galaxies not accessible in standard observation. Indeed, the natural magnification due to massive galaxy clusters allows to spatially resolve and constrain the dynamics of star forming galaxies 1 to 3 mags fainter than those selected in blank fields. Finally, multiplexed-IF spectroscopy is the natural next step in galaxy surveys. The extra information gained by IFU spectroscopy, combined with the statistical power of a large survey, will enable a fundamental step forward by distinguishing the spectroscopic properties of the major structural components of galaxies. There is no doubt that IFU-based science from future observatories like TMT will transform our understanding of many features of the physics of galaxy formation and evolution.*